Iranian Journal of Basic Medical Sciences

ijbms.mums.ac.ir

IJBMS

Gold-gold sulfide nanoshell as a novel intensifier for anti-tumor effects of radiofrequency fields

Hamid Reza Sadeghi [1], Mohammad Hossein Bahreyni-Toosi [2], Naser Tayebi Meybodi [3], Habibollah Esmaily [4], Samaneh Soudmand [1], Hossein Eshghi [5], Ameneh Sazgarnia [1*]

[1] Medical Physics Research Center, Mashhad University of Medical Sciences, Mashhad, Iran
[2] Medical Physics Research Center, Mashhad University of Medical Sciences, Mashhad, Iran
[3] Department of Pathology, Imam Reza Hospital, Mashhad University of Medical Sciences, Mashhad, Iran
[4] Department of Biostatistics, Faculty of Health Sciences, Mashhad University of Medical Sciences, Mashhad, Iran
[5] Department of Chemistry, School of Sciences, Ferdowsi University of Mashhad, Mashhad, Iran

ARTICLE INFO

Article type:
Original article

Article history:
Received: Sep 10, 2013
Accepted: Apr 19, 2014

Keywords:
Au-Au_2S
BALB/c mice
CT26 cells
Gold-gold sulfide
Radiofrequency Field

ABSTRACT

Objective(s): Several studies have been carried out to investigate the effect of various nanoparticles exposed to radiofrequency (RF) waves on cancerous tissues. In this study, a colon carcinoma tumor model was irradiated by RF in the presence of gold-gold sulfide (GGS) nanoshells.

Materials and Methods: Synthesis and characterization of GGS nanoshells were initially performed. CT26 cells were subcutaneously injected into the flank of BALB/c mice to create the colon carcinoma tumor models. Then the tumors were subjected to different treatments. Treatment factors included intratumoral injection of GGS and RF radiation. Different groups were considered as control with no treatment, receiving GGS, RF irradiated and simultaneous administration of GGS and RF. Efficacy of the treatments was evaluated by daily monitoring of tumor volume and recording the relative changes in it, the time needed for a 5-fold increase in the volume of tumor (T_5) and utilizing pathologic studies to determine the lost volume of the tumors.

Results: In comparison with control group, tumor growth was not markedly inhibited in the groups receiving only GGS or RF, while in the group receiving GGS and RF, tumor growth was effectively inhibited compared with the other groups. In addition, the lost volume of the tumor and T_5 was markedly higher in groups receiving GGS and RF compared with other groups.

Conclusion: This study showed that RF radiation can markedly reduce the tumor growth in presence of GGS. Hence, it can be predicted that GGS nanoshells convert sub-lethal effects of noninvasive RF fields into lethal damages.

► *Please cite this paper as:*
Sadeghi HR, Bahreyni-Toosi MH, Tayebi Meybodi N, Esmaily H, Soudmand S, Eshghi H, Sazgarnia A. Gold-gold sulfide nanoshell as a novel intensifier for anti-tumor effects of radiofrequency fields. Iran J Basic Med Sci 2014; 17:516-521.

Introduction

Compared to bulk materials of the same substance, nanostructures attain a larger surface to volume ratio due to their small size and volume. The high surface to volume ratio, especially in metallic nanostructures, results in utterly different and sometimes unknown electrical, magnetic and optical properties (1, 2). For example, gold nanostructures (including nanoparticles, nanorods and nanoshells) are able to absorb the energy of laser radiation in the near infrared (NIR) region and efficiently convert it to heat (3). As gold nanostructures are biocompatible, the heat can be utilized in medical applications to damage malignant cells and to treat cancer (photothermal therapy) (4). The main problem of these treatments in practice is low penetration depth of the laser (3, 5). In addition to NIR lasers, other sources of electromagnetic spectrum such as radiofrequency generators are used for various purposes in medicine (6). Non-invasive and non-ionizing radiofrequency waves are able to penetrate deep into the tissues; therefore, they can theoretically be applied to the tissues in any part of the body. Electromagnetic waves at frequencies of 13.56 and 27.12 MHz have been previously used to induce hyperthermia effects as an adjuvant treatment together with radiotherapy or chemotherapy (6-8).

*Corresponding author: Ameneh Sazgarnia. Medical Physics Research Center, Mashhad University of Medical Sciences, Mashhad, Iran. Tel: +98-511-8002323; Fax: +98-511-8002320; email: Sazgarniaa@mums.ac.ir

The main problem in using RF waves is non-selectivity of tumor tissue as a target rather than surrounding healthy non-target tissues and its almost identical absorption in these tissues (9, 10). Over the past few years, several research groups have considered the targeted treatment of cancer cells by using RF radiation as primary treatment. They have done this by accumulating different nano-particles in malignant tissues (9-12). In this regard, some *in vitro* and *in vivo* studies have been conducted using gold nanostructures exposed to RF radiation. The results show more efficient apoptosis of target tissues compared to healthy tissue (13-15). There are theoretical debates about the reasons for these findings. However, it is not clear whether the heat produced via RF absorption by nanoparticles kills the target cells or direct biological effects of RF radiation, which are sub-lethal, become fatal in presence of nano-particles (16-18). Nevertheless, *in vitro* and *in vivo* studies on different cell lines have been repeated, and the results demonstrate the additional effectiveness of gold nanostructures and RF fields in targeted destruction of cancer cells (19, 20). However, according to the latest findings, the absorption of RF wave energy has been found to increase, provided that overall diameter of the particles is less than 10 nm (16, 21). The absorption of energy was also intensified by shell structure of the particles (22). Au-Au_2S (GGS) is a gold nanoshell with such features (23). GGS presence with exposure to RF radiation is expected to cause targeted killing of malignant cells effectively. GGS structure consists of a dielectric core made of gold sulfide with a thin shell of gold. The nanoshells can be synthesized by a very simple, cheap and controllable method, in contrast with similar morphological nanostructures (24). Nanoshells with diameters generally less than 10 nm can also be synthesized. In addition, GGS similar to gold nanoparticle does not cause acute or chronic toxicity, easily penetrates the cells and can bind targeting agents (e.g. antibodies, peptides or pharmacological agents) (25, 26). This study has investigated the *in vivo* effects of GGS exposed to RF radiation on the CT26 tumor model.

Materials and Methods

Synthesis and characterization of GGS

By mixing aqueous solutions of $HAuCl_4$ (Alfa Aesar, USA) and Na_2S (Merck, Germany), GGS was grown (24). In fact, 20 ml of 2 mM $HAuCl_4$ was mixed with 20 ml of 1 mM Na_2S, and stored at 25˚C for 1 day. A UV-visible spectrophotometer (UV 1700, Shimadzu Corp., Japan) was used to monitor the reaction at the wavelength range of 200-900 nm. After preparing the nanoparticles, 0.6 g polyvinylpyrrolidone (PVP; $(C_6H_9NO)n$) was added to prevent nanoparticles aggregation. Finally, to purify GGS nanoshells, the particles were completely separated using sequential centrifugation procedure (27).

Then, we utilized transmission electron microscopy (TEM) (CM 120, Philips, Germany) operating at acceleration voltage of 120 kV to examine the morphology of GGS. The size distribution of the nanoparticles was determined by means of a particle size analyzer (Zetasizer, Malvern Ins., USA). Furthermore, we exploited the UV-visible spectrophotometer in order to record the GGS UV-visible absorption spectrum.

Cell lines and culture conditions

CT26 cell line (Pasteur Inst., Iran) derived from colon carcinoma of a BALB/c mouse was grown in RPMI-1640 (Gibco, Life Technologies Corp., USA) supplemented with 10% (v/v) fetal bovine serum (FBS), 100 units/ml penicillin and 100 µg/ml streptomycin. Cell culture was performed at 37˚C in a 5% CO_2 humidified incubator (NU 8500, NuAire Corp., USA). The cells covered the bottom of the flask as a monolayer after 2-3 days of cell growth and proliferation. Exponentially growing cells were trypsinized using 0.05% trypsin-EDTA. The cell count and survival rate were determined by a hemocytometer using trypan blue staining.

Tumor model

Inbred 4-6 week BALB/c male mice weighting about 20 g were purchased from Iranian Pasteur Institute and kept under standard conditions of temperature, humidity, lighting and feeding in an animal house. In order to induce tumor models, the animals were subcutaneously injected by 5×10^5 viable CT26 cells suspended in 150 µl normal saline in the right flank. As the tumor volume reached approximately 100 mm^3 (10 days after injection), 5 mice were randomly sacrificed, autopsied and were subjected to the pathological examinations, and the presence of tumor was confirmed.

Anesthetizing the animals

To prevent animal movement during treatment, the mice were anesthetized before treating. For this purpose, 6 mg/kg Xylazine and 60 mg/kg Ketamine was injected intraperitoneally.

RF generator

We adapted variable power RF (at the frequency of 13.56 MHz) signal generator (Model 800 Crystal Brandmaster, Britcher Corp, USA) for our purposes in this test. The generating machine consisted of a power generator and adjustable distance transmitting/receiving couplers. A Spectrum Analyzer (HP 8566B, Hewlett-Packard, USA) was connected to the system to measure transmitted power. The process of impedance matching during RF exposure was so advantageous for monitoring and minimizing the reflected RF power.

Treatment protocol

48 tumor bearing mice were randomly divided into four groups. In each group, there were 7 mice for follow-up and 5 mice for pathological studies. The groups were as follows: Group 1: control, Group 2: receiving GGS, Group 3: receiving RF radiation and Group 4: receiving GGS with RF radiation. The mice in groups 2 and 4 were intratumorally injected by 1 mg/kg GGS directly around various points of the tumor (28-30). Groups 3 and 4 were irradiated by 400W-power RF radiation for 4 min. To do this, the completely shaved region of tumor was placed between transmitter/receiver plates of RF signal generator. The plates were fully insulated to prevent electrical discharge and shock. In Group 4, the irradiation was performed 20 min after injection of the GGS (28-30).

Assessment of therapeutic efficacy

7 mice per group were considered for follow-up treatment. Monitoring the effects of treatments was performed by daily measurement of tumor diameters, including small diameter (a), large diameter (b) and thickness of tumor (c) using a digital vernier caliper with accuracy of 0.01 mm. The volume of tumors (V) was estimated using equation (1):

$$V = \pi/6(a \cdot b \cdot c) \quad (1)$$

The monitoring continued for 40 days after treatment. The treatment day was considered as a reference in order to do the final comparison; the relative tumor volume on all days was normalized to the volume on the reference day. According to the daily changes in relative tumor volume, the time needed for a 5-fold increase in tumor volume (T_5) was determined by regression analysis in each group. Five mice per group were considered for histopathological studies. The pathologic examinations revealed the percentage of necrosis in each tumor 24 hr after treatment day. Using these results, reduction in volume of tumor tissue was estimated 24 hr after treatment.

In order to perform histologic examinations on tumors and evaluate the changes resulting from the treatments, 5 animals in each group were sacrificed, and the tumors were autopsied. Microscopic slides prepared from tumor tissues were studied by a single pathologist who was blinded to the treatment protocol, and the percentage of necrosis was reported.

Statistical analysis of the data

All data were analyzed using SPSS 12 after performing normality test and selecting the proper comparative tests. According to the normality test of Kolmogorov-Smirnov, the data distribution was normal. Therefore, one-way ANOVA with a confidence level of 95% was used to compare the data. Mutual comparisons between groups were performed using Tukey test.

Results

GGS characterization

Figure 1 illustrates the diagram of particle size analysis (PSA) using dynamic light scattering (DLS) method with a peak at 5.4 nm. PDI (polydispersity index) was determined as 0.63. TEM image of the synthesized samples has been shown in Figure 2. In UV-Vis spectroscopy of the synthesized samples, a strong absorption band was observed at 759 nm in the NIR region and a weak absorption band was seen at 529 nm in the visible region, which confirms synthesis of GGS nanoshells (23-24).

Assessment of therapeutic efficacy

Figure 3 shows the changes in relative volume of tumors in different groups until 4 weeks after treatment.

No growth inhibiting effect was observed in tumor volume of control and GGS receiving groups. Tumor growth became slow in the RF irradiated group compared with the control group, but this effect was significantly more pronounced in GGS+RF group. Statistical analysis showed that on 10, 15, 20 and 25 days after treatment, there was no statistically significant difference between relative volume of tumor in control group compared to GGS

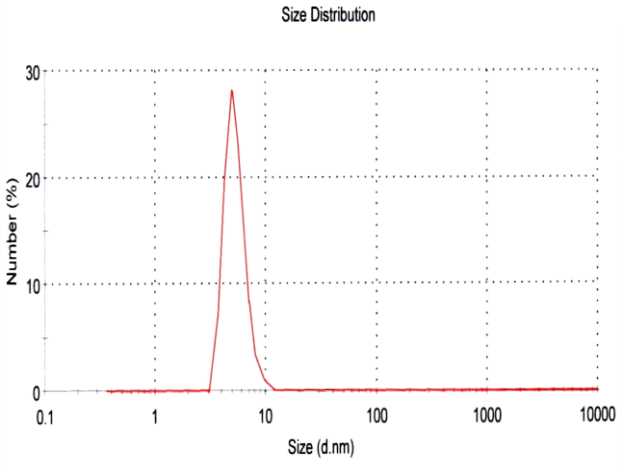

Figure 1. Size distribution of synthesized gold- gold sulfide nanoshells (maximum abundance of particles distribution at 5.4 nm)

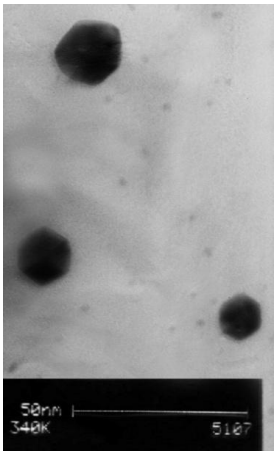

Figure 2. A TEM image of synthesized gold-gold sulfide nanoshells

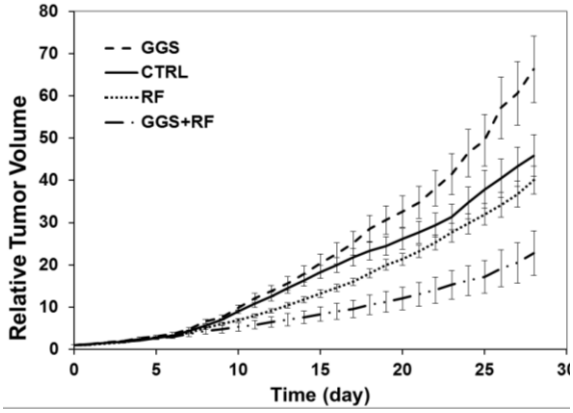

Figure 3. Mean ± standard error of relative volume of tumors until 4 weeks after treatment in the different groups (10 mice in each group). Control group shows growth of untreated tumors. GGS group is a group of tumors injected with GGS. Tumors of RF group were only exposed to radiofrequency fields. The group of GGS+RF is group of tumors irradiated by radiofrequency fields 10 min after intratumoral injection of 1 mg/kg gold-gold sulfide. Radiofrequency exposures were performed for 4 min

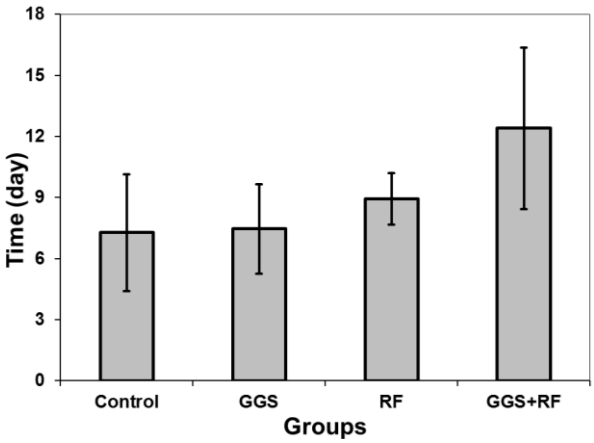

Figure 4. Time required for 5-fold increase in tumor volume (T_5) of different groups. Data represent the mean of T_5 obtained from 10 tumor models in each group ± standard error on the mean

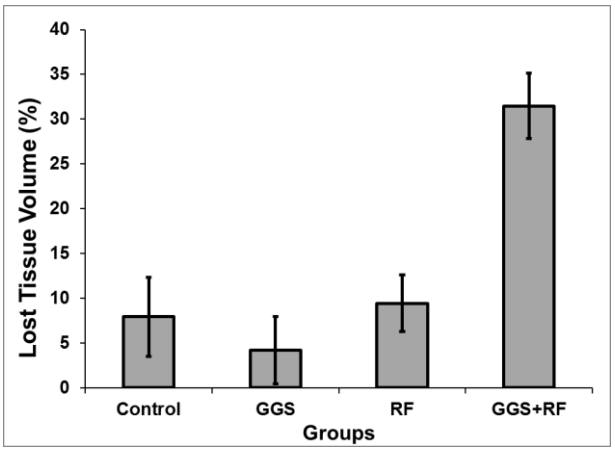

Figure 5. Percentage of lost tissue 24 hrs_after treating different groups. Data represent the mean of lost tumor volume percentage estimated for 5 tumors in each group ± standard error on the mean

group and also RF group (P=0.072). But during all these days, relative volume of tumors in GGS+RF group was significantly with GGS and control groups (P<0.001). However, no significant difference was observed between the relative volume of tumors in GGS+RF group and that in RF group (P=0.217).

Figure 4 shows the time required for a 5-fold increase in tumor volume in different groups.

The minimum and maximum T_5 were determined as 7.3 and 12.4 days for control and GGS+RF receiving groups, respectively. Statistical analysis showed no significant difference between T_5 of the control group and that of GGS and RF groups (P=0.789). However, the difference between GGS+RF group and control or GGS groups were statistically significant (P<0.012). However, the T_5 between GGS+RF group and RF group was not statistically significant (P=0.157). Figure 5 illustrates volume of the lost tumor tissue in terms of percentage of total volume for different groups, according to the pathological findings.

The lowest volume of lost tissue was calculated for GGS group as 4.2% and the highest volume was that of GGS+RF group with 31.5%. Statistical analysis showed that the differences between percentage of lost tissue volume in control, GGS and RF groups were not significant (P=0.902). However, significant differences between all groups in comparison with the GGS+RF group has been observed (P<0.013).

Discussion

Recently, the use of RF radiation together with nanoparticles (especially gold nanoparticles) has been noticed and discussed in order to induce lethal damage in malignant tissues. Present study also indicates the relative tumor volume was significantly reduced in the treatment group (GGS+RF waves) in comparison with the control group. These results are in agreement with the findings of Cardinal *et al* and Curley *et al*. However, the origins and mechanisms of

damage to malignant tissue are not clearly identified. Based upon Moran *et al* studies, it seems that gold nanoparticles with diameters less than 50 nm cause a sudden rise in ambient temperature via energy absorption of RF and heat generation (22). As a result, by inserting the nanoparticles within the cancer cells and exposing them to RF radiation, irreversible damage can be inflicted to these cells, while due to the absence of nanoparticles in healthy tissues, these tissues suffer no harm. However, further detailed studies of Li *et al* have shown that the heat is due to ionic impurities associated with nanoparticles (17). To reduce the effect of such factors, we purified nanoparticles according to Gobin *et al* (27). Having removed the impurities, San *et al* and Corr *et al* determined that the diameter of nanoparticles should be less than 10 nm to generate suitable heat (16, 21). GGS nanoshells used in this study had these features and were prepared under such conditions. In contrast with other gold nanoshells, GGS nanoshells in sizes smaller than 10 nm are easily and inexpensively synthesized. GGS injection creates no specific toxicity in animals. In this study, neither mortality nor other significant side effects have been observed in the GGS receiving group, like all other groups for 40 days after treatment, although no evidence of reduction in tumor volume was observed in the GGS group. In contrast, relative reduction in tumor volume was observed in the RF group, although this reduction was not significant compared to the control group, but also not negligible. Recent theoretical bioelectric studies of Iomin and experimental research of Palti *et al* suggest that RF waves have the ability to interrupt or interfere with the cell cycle (31-33). Stupp *et al* have even utilized this phenomenon clinically for the treatment of GBM (34). In addition, RF radiation to conductor environments such as living tissues inevitably induces high-frequency microcurrents. The presence of these microcurrents also impairs cellular processes (32, 33). According to the above-mentioned reasons, reduction in relative volume of tumor RF seems to be justified. Moreover, recent studies of Raoof *et al* have shown that inherent permittivity of malignant tissues is more than that of normal tissues in the range of RF waves (18). However, RF waves cause temperature rise in malignant tissues compared to healthy tissues, after being exposed to RF radiation. This means that even without the presence of nanoparticles, it is expected that damage to malignant tissues be greater than to healthy tissues with RF radiation (18). In this study, based on statistical analysis, this decline in tumor volume cannot be considered as an effective phenomenon in preventing tumor growth. However, based on theoretical studies of Tiwari *et al*, interruption or disruption of cell cycle due to RF waves was obviously increased in presence of nanoparticles, which disrupt space symmetry of living cells (35). In this way, we can state another reason for obvious reduction in volume of tumor in GGS+RF compared to RF group. In the present study, regardless of the hyperthermic justification for the reduction in volume of tumor in GGS+RF group, it seems that GGS presence in the cells enhances the effect of RF radiation in stopping growth of the tumor. Based upon the reasons stated above, it seems that the presence of GGS biocompatible nanoshells in tumor cells perceptibly raises the thermal sub-lethal or bioelectric effects of RF, and these effects in turn inhibit tumor growth. The results of needed time for a 5-fold increase in volume of tumor also endorse the reasons. However, the results of lost tumor volume indicate significant differences for relative volume of tumor in GGS+RF group compared with all other groups, even irradiated RF group. In addition, it seems that the difference among the different treated groups gets stronger after 24 hr. However, over time and with proliferation of the tumor cells, this difference is blurred. As the damaging mechanisms usually act at the cellular level, causing no drastic genetic changes, reconstruction of tumor is not surprising over time. To get more definite results, we need fractionation of similar treatments with fractionated doses of ionizing radiation (18). However, more comprehensive radiobiological studies in this field seem to be necessary.

Conclusion

In this study, RF waves in the absence of GGS caused no effective reduction in volume of the tumor. However, the GGS nanoshells in tumors exposed to noninvasive RF radiation decrease growth of the tumors. Although this was not the first time the simultaneous impact of nanoparticles and RF waves was observed, using GGS as a biocompatible as well as accessible and inexpensive nanoshell is a novelty.

Acknowledgment

This study was financially supported by Research Department of Mashhad University of Medical Sciences, Mashhad, Iran. The results described in this paper are a part of a PhD student thesis.

References

1. Bhattacharyya S, Kudgus RA, Bhattacharya R, Mukherjee P. Inorganic nanoparticles in cancer therapy. Pharm Res 2011; 28:237-259.
2. Hirsch LR, Gobin AM, Lowery AR, Tam F, Drezek RA, Halas NJ, *et al*. Metal nanoshells. Ann Biomed Eng 2006; 34:15-22.
3. Huang X, Jain PK, El-Sayed IH, El-Sayed MA. Plasmonic photothermal therapy (PPTT) using gold nanoparticles. Lasers Med Sci 2008; 23:217-228.
4. Cobley CM, Chen J, Cho EC, Wang LV, Xia Y. Gold nanostructures: a class of multifunctional materials for biomedical applications. Chem Soc Rev 2011; 40:44-56.

5. Huang X, El-Sayed MA. Gold nanoparticles: Optical properties and implementations in cancer diagnosis and photothermal therapy. J Adv Res 2008; 1:13-28.
6. D'Andrea JA, Ziriax JM, Adair ER. Radio frequency electromagnetic fields: mild hyperthermia and safety standards. Prog Brain Res 2007; 162:107-135.
7. Habash RW, Bansal R, Krewski D, Alhafid HT. Thermal therapy, part 2: hyperthermia techniques. Crit Rev Biomed Eng 2006; 34:491-542.
8. Chou C-K. Application of electromagnetic energy in cancer treatment. IEEE T instrum Meas 1988; 37:547-551.
9. Cherukuri P, Curley SA. Use of nanoparticles for targeted, noninvasive thermal destruction of malignant cells. Methods Mol Biol 2010; 624:359-373.
10. Cherukuri P, Glazer ES, Curley SA. Targeted hyperthermia using metal nanoparticles. Adv Drug Deliv Rev 2010; 62:339-345.
11. Glazer ES, Curley SA. Non-invasive radiofrequency ablation of malignancies mediated by quantum dots, gold nanoparticles and carbon nanotubes. Ther Deliv 2011; 2:1325-1330.
12. Glazer ES, Curley SA. Radiofrequency field induced thermal cytotoxicity in cancer cells treated with fluorescent nanoparticles. Cancer 2010; 116:3285-3293.
13. Glazer ES, Zhu C, Massey KL, Thompson CS, Kaluarachchi WD, Hamir AN. Noninvasive radiofrequency field destruction of pancreatic adenocarcinoma xenografts treated with targeted gold nanoparticles. Clin Cancer Res 2010; 16:5712.
14. Raoof M, Curley SA. Non-invasive radiofrequency-induced targeted hyperthermia for the treatment of hepatocellular carcinoma. Int J Hepatol 2011; 6.
15. Cardinal J, Klune JR, Chory E, Jeyabalan G, Kanzius JS, Nalesnik M, *et al.* Noninvasive radiofrequency ablation of cancer targeted by gold nanoparticles. Surgery 2008; 144:125-132.
16. Corr SJ, Raoof M, Mackeyev Y, Phounsavath S, Cheney MA, Cisneros BT, *et al.* Citrate-capped gold nanoparticle electrophoretic heat production in response to a time-varying radio-frequency electric field. J Phys Chem C 2012; 116:24380-24389.
17. Li D, Jung YS, Tan S, Kim HK, Chory E, Geller DA. Negligible absorption of radiofrequency radiation by colloidal gold nanoparticles. J Colloid Interface Sci 2011; 358:47-53.
18. Raoof M, Cisneros BT, Corr SJ, Palalon F, Curley SA, Koshkina NV. Tumor selective hyperthermia induced by short-wave capacitively-coupled RF electric-fields. PloS One 2013.
19. Raoof M, Zhu C, Kaluarachchi WD, Curley SA. Luciferase-based protein denaturation assay for quantification of radiofrequency field-induced targeted hyperthermia: developing an intracellular thermometer. Int J Hyperthermia 2012; 28:202-209.
20. Raoof M, Corr SJ, Kaluarachchi WD, Massey KL, Briggs K, Zhu C. Stability of antibody-conjugated gold nanoparticles in the endolysosomal nanoenvironment: implications for noninvasive radiofrequency-based cancer therapy. Nanomedicine 2012; 8:1096-1105.
21. San BH, Moh SH, Kim KK. Investigation of the heating properties of platinum nanoparticles under a radiofrequency current. Int J Hyperthermia 2013; 29:99-105.
22. Moran CH, Wainerdi SM, Cherukuri TK, Kittrell C, Wiley BJ, Nicholas NW. Size-dependent joule heating of gold nanoparticles using capacitively coupled radiofrequency fields. Nano Res 2009; 2:400-405.
23. Tan MC, Ying JY, Chow GM. Composition, particle size, and near-infrared irradiation effects on optical properties of Au-Au_2S nanoparticles. J Mater Res 2008; 23:281-293.
24. Ren L, Huang XL, Zhang B, Sun LP, Zhang QQ, Tan MC, *et al*. Cisplatin-loaded Au-Au2S nanoparticles for potential cancer therapy: Cytotoxicity, *in vitro* carcinogenicity, and cellular uptake. J Biomed Mater Res A 2008; 85A:787-796.
25. Tan MC, Ying JY, Chow GM. Interfacial properties and *in vitro* cytotoxic effects of surface-modified near infrared absorbing Au-Au_2S nanoparticles. J Mater Sci-Mater M 2009; 20:2091-2103.
26. Huang X-L, Zhang B, Ren L, Ye S-F, Sun L-P, Zhang Q-Q. *In vivo* toxic studies and biodistribution of near infrared sensitive Au–Au_2S nanoparticles as potential drug delivery carriers. J Mater Sci Mater Med 2008; 19:2581-2588.
27. Gobin AM, Watkins EM, Quevedo E, Colvin VL, West JL. Near infrared resonant gold/gold sulfide nanoparticles as a photothermal cancer therapeutic agent. Small 2010; 6:745-752.
28. Kennedy LC, Bickford LR, Lewinski NA, Coughlin AJ, Hu Y, Day ES, *et al*. A new era for cancer treatment: Gold-nanoparticle-mediated thermal therapies. Small 2011; 7:169-183.
29. Chen H, Zhang X, Dai S, Ma Y, Cui S, Achilefus S, *et al*. Multifunctional Gold Nanostar Conjugates for Tumor Imaging and Combined Photothermal and Chemo-therapy. Theranostics 2013; 3:633-649.
30. Al-Ghananeem AM, Malkawi AH, Muammer YM, Balko JM, Black EP, Mourad W. Intratumoral delivery of paclitaxel in solid tumor from biodegradable hyaluronan nanoparticle formulations. Aaps Pharmscitech 2009; 10:410-417.
31. Iomin A. A toy model of fractal glioma development under RF electric field treatment. Eur Phys J E. 2012; 35:1-6.
32. Giladi M, Porat Y, Blatt A, Shmueli E, Wasserman Y, Kirson ED, *et al*. Microbial growth inhibition by alternating electric fields in mice with Pseudomonas aeruginosa lung infection. Antimicrob Agents Chemother 2010; 54:3212-3218.
33. Palti Y, Schneiderman RS, Shmueli E, Kirson ED. TTFields alone and in combination with chemotherapeutic agents effectively reduce the viability of MDR cell sub-lines that over-express ABC transporters. BMC Cancer 2010; 10:229.
34. Stupp R, Wong ET, Kanner AA, Steinberg D, Engelhard H, Heidecke V. NovoTTF-100A versus physician's choice chemotherapy in recurrent glioblastoma: a randomised phase III trial of a novel treatment modality. Eur J Cancer 2012; 48:2192-2202.
35. Tiwari PK, Kang SK, Kim GJ, Choi J, Mohamed A, Lee JK. Modeling of nanoparticle-mediated eectric field enhancement inside biological cells exposed to AC electric fields. Japan J Appl Phys 2009; 48:087001.